

Transiting Extrasolar Planet with a Companion: Effects of Orbital Eccentricity and Inclination

Masanao SATO, and Hideki ASADA

Faculty of Science and Technology, Hirosaki University, Hirosaki, Aomori 036-8561

(Received ; accepted)

Abstract

Continuing work initiated in an earlier publication [Sato and Asada, PASJ, 61, L29 (2009)], we consider light curves influenced by the orbital inclination and eccentricity of a companion in orbit around a transiting extrasolar planet (in a planet-satellite system or a hypothetical true binary). We show that the semimajor axis, eccentricity and inclination angle of a ‘moon’ orbit around the host planet can be determined by transit method alone. For this purpose, we present a formulation for the parameter determinations in a small-eccentricity approximation as well as in the exact form. As a result, the semimajor axis is expressed in terms of observables such as brightness changes, transit durations and intervals in light curves. We discuss also a narrow region of parameters that produce a mutual transit by an extrasolar satellite.

Key words: techniques: photometric — eclipses — occultations — planets and satellites: general — stars: planetary systems

1. Introduction

It is of general interest to discover a second Earth-Moon system. Detections of such an extrasolar planet with a satellite (or hypothetical binary planet systems that do not exist in the Solar System) and probing the nature of such objects will bring important information to planet (and satellite) formation theory (e.g., Williams et al. 1997, Jewitt and Sheppard 2005, Canup and Ward 2006, Jewitt and Haghighipour 2007). If a giant planet with a (perhaps Earth-size) rocky satellite were located at a certain distance from their host star, the satellite may be habitable and show vegetation, though these issues are out of the scope of this paper.

It is not clear whether the IAU definition for planets in the Solar System can be applied to extrasolar planets as it is. The IAU definition in 2006 is as follows: A planet is a celestial body that (a) is in orbit around the Sun, (b) has sufficient mass so that it assumes a hydrostatic equilibrium (nearly round) shape, and (c) has cleared the neighborhood around its orbit.

Regarding (c), the Earth can be called a planet, mostly because the common center of

mass (COM) of the Earth-moon system is below the surface of the Earth. On the other hand, the COM of the Pluto-Charon system is located above the surfaces of these objects. Therefore, it is interesting to determine the COM position of a planet-companion system. In order to determine it, we have to know the true (not apparent) distance between the two objects. For this reason, Sato and Asada (2009) considered extrasolar mutual transits, as a complementary method of measuring not only the radii of two transiting objects but also their separation (See Sato and Asada 2009 also on detection probabilities of extrasolar mutual transits and a possible limit by Kepler Mission). As a particular case, a short separation binary, which has a rapidly orbiting companion, gives us a unique opportunity to measure the true separation of the binary, whereas a long separation one gives us only the apparent separation. Their work is very limited, however, in the sense that they assume circular orbits and also coplanar orbits as $I = 90$ degrees for both planet and moon. Clearly it is important to take account of the orbital inclination and eccentricity. The main purpose of this paper is to study effects of the orbital inclination and eccentricity of a companion on extrasolar mutual transits.

Since the first detection of a transiting extrasolar planet (Charbonneau et al. 2000), photometric techniques have been successful (e.g., Deming et al. 2005 for probing atmosphere, Ohta et al. 2005, Winn et al. 2005, Gaudi & Winn 2007, Narita et al. 2007, 2008 for measuring spin-orbit alignment angle). In addition to *COROT*¹, *Kepler*² is monitoring about 10^5 stars with expected 20 ppm ($= 2 \times 10^{-5}$) photometric differential sensitivity for stars of $V=12$. This will marginally enable the detection of a moon-size object. In fact, *COROT* detected a transiting super-Earth (Leger et al. 2009, Queloz et al. 2009).

Sartoretti and Schneider (1999) first suggested a photometric detection of extrasolar satellites. Cabrera and Schneider (2007) developed a method based on the imaging of a planet-companion as an unresolved system (but resolved from its host star) by using planet-companion mutual transits and mutual shadows. As an alternative method, timing offsets for a single eclipse have been investigated for eclipsing binary stars as a perturbation of transiting planets around the center of mass in the presence of the third body (Deeg et al. 1998, 2000, Doyle et al. 2000). It has been recently extended toward detecting ‘exomoons’ (Szabó et al. 2006, Simon et al. 2007, Kipping 2009a, 2009b). Sato and Asada (2009) investigated effects of mutual transits by an extrasolar planet with a companion on light curves. In particular, they studied how the effects depend on the companion’s orbital velocity. Furthermore, extrasolar mutual transits were discussed as a complementary method of measuring the system’s parameters such as a planet-companion’s separation and thereby of identifying them as a true binary, planet-satellite system or others.

Their method has analogies in classical ones for eclipsing binaries (e.g., Binnendijk 1960, Aitken 1964). A major difference is that occultation of one faint object by the other transiting

¹ <http://www.esa.int/SPECIALS/COROT/>

² <http://kepler.nasa.gov/>

a parent star causes an apparent *increase* in light curves, whereas eclipsing binaries make a decrease. What is more important is that, in both cases where one faint object transits the other and vice versa, changes are made in the light curves due to mutual transits even if no light emissions come from the faint objects. In a single transit, on the other hand, thermal emissions from a transiting object at lower temperature make a difference in light curves during the secondary eclipse, when the object moves behind a parent star as observed for instance for HD 209458b (Deming et al. 2005).

This paper is organized as follows. In section 2, we consider effects of the orbital inclination and eccentricity of a companion on light curves. For simplicity, henceforth, such a companion orbiting around a host planet is called a ‘moon’ even if it is not a satellite but a component of a hypothetical binary planet. In section 3, we present a formulation for parameter determinations. Some numerical examples are also presented. Section 4 is devoted to the conclusion.

2. Effects of the Orbital Eccentricity of a Transiting ‘Moon’ on Light Curves

2.1. Approximations and notation

The time duration of a transit, say a few hours, is much longer than the orbital period of an extrasolar planet, say a few days or greater. In one transit, the effect of the motion of the moon is much larger than that of the planet orbiting around a star. During the transit, therefore, we employ a constant velocity approximation only for the orbital motion of a planet-moon system around their host star. For a short separation case, on the other hand, we take account of the eccentric orbit of the moon, because the orbital period of such a moon around the planet may be comparable to (or shorter than) the timescale of the transit.

The co-planar assumption that the orbital plane of a moon around its primary object is the same as that of the planet in orbit around the host star seems reasonable because it seems that planets are born from fragmentations of a single proto-stellar disk and thus their spins and orbital angular momentum are nearly parallel to the spin axis of the disk. Irregular satellites such as Triton, however, have significant inclinations presumably through capture processes. This requires that we should include the effect of orbital inclinations. We assume only the moon’s orbital inclination, because it makes substantial effects on mutual transit light curves. Inclinations of the planet’s orbital plane have been well understood and already observed (Charbonneau et al. 2000).

Here we list our assumptions for clarity.

- The inclination angle of the COM of the planet and moon is fixed at 90 degrees.
- We take account of the inclination angle of the moon’s orbit.
- We assume that the planet-moon COM has a constant velocity (during a transit by the planet in front of the host star).

- The longitude of ascending node of the moon equals zero.
- The planet-moon COM orbit has zero eccentricity.
- We assume no limb darkening effects.

For an eccentric orbit, we generally have the Kepler equation as

$$t = t_0 + \frac{T}{2\pi}(u - e \sin u), \quad (1)$$

where t_0 , T , e and u denote the time of periastron passage, orbital period, eccentricity and eccentric anomaly, respectively (e.g., Danby 1988, Roy 1988, Murray and Dermott 1999). In the following, we use the true anomaly f instead of the eccentric anomaly u (e.g., Danby 1988, Roy 1988, Murray and Dermott 1999). They are related by

$$\tan \frac{f}{2} = \sqrt{\frac{1+e}{1-e}} \tan \frac{u}{2}. \quad (2)$$

The distance between the orbiting body and a focus of the ellipse is written as

$$r = \frac{a(1-e^2)}{1+e \cos f}. \quad (3)$$

We use these equations for describing a moon orbiting around a planet. We denote the mean motion of the moon in orbit around the primary as $n_m \equiv 2\pi/T_m$, where the subscript m means the moon's quantity. The subscript p denotes the planet's quantity.

For investigating transits, we need the transverse position x and velocity v of each object. We denote those of the COM for planet-moon systems as x_{CM} and v_{CM} , respectively, where the origin of x is chosen as the center of the star. We assume v_{CM} as constant during the transit. The position and velocity of each planet with mass M_p and M_m in the planet-moon system as x_i and v_i ($i = p, m$), respectively. The direction of the observer's line of sight is specified by the argument of pericenter as an angle denoted by ω_m (See also Fig. 1). We express the transverse position as

$$x_{CM} = v_{CM}(t - t_{CM}), \quad (4)$$

$$x_p = x_{CM} + a_p[(\cos u - e_m) \cos \omega_m + \sqrt{1-e_m^2} \sin u \sin \omega_m], \quad (5)$$

$$x_m = x_{CM} - a_m[(\cos u - e_m) \cos \omega_m + \sqrt{1-e_m^2} \sin u \sin \omega_m], \quad (6)$$

where the semimajor axis of the orbit of each object around their COM is denoted by a_i , and t_{CM} means the time when the binary's common center of mass passes in front of the center of the host star. In terms of the true anomaly, they are rewritten as

$$x_p = x_{CM} + a_p \frac{(1-e_m^2) \cos(f + \omega_m)}{1+e_m \cos f}, \quad (7)$$

$$x_m = x_{CM} - a_m \frac{(1-e_m^2) \cos(f + \omega_m)}{1+e_m \cos f}. \quad (8)$$

(See Table 1 for a list of parameters and their definition).

The azimuthal velocity of the secondary object around the primary is

$$\begin{aligned}
V_f &= r \frac{df}{dt} \\
&= a_{pm} n_m \frac{1 + e_m \cos f}{\sqrt{1 - e_m^2}},
\end{aligned} \tag{9}$$

where f denotes the true anomaly (Murray and Dermott 2000). Here, a_{pm} and e_m denote the semimajor axis and eccentricity of the moon’s orbit with respect to the host planet. We assume that both the eccentricity of COM orbit vanishes and the inclination angle of COM equals 90 degrees. Hence we can avoid a careful treatment of “sky-projected transverse position”.

2.2. Transits in light curves

We denote the intrinsic stellar luminosity as L . The apparent luminosity L' due to mutual transits is expressed as

$$L' = L \times \frac{S - \Delta S}{S}, \tag{10}$$

where $S = \pi R_s^2$, $S_p = \pi R_p^2$, $S_m = \pi R_m^2$, $\Delta S = S_p + S_m - S_{pm}$. Here, R_s , R_p and R_m denote the radii of the host star, planet and moon, and S_{pm} denotes the area of the apparent overlap between them, which is seen from the observer. Without loss of generality, we assume that the primary is larger than the secondary as $R_p \geq R_m$.

2.3. Effects on light curves

We investigate light curves by mutual transits due to planet-moon systems. The orbital velocity is of the order of $a_{pm} n_m$. Therefore, we have two cases; $v_{CM} < a_{pm} n_m$ and $v_{CM} > a_{pm} n_m$.

The dimensionless ratio of the moon’s orbital velocity to the planet’s one is defined as

$$W \equiv \frac{a_{pm} n_m}{v_{CM}}. \tag{11}$$

If $v_{CM} < a_{pm} n_m$, we call it a fast case. If $v_{CM} > a_{pm} n_m$, we call it a slow one. The Earth-Moon ($W = 0.03$), Jupiter-Ganymede ($W = 0.8$) and Jupiter-Io ($W = 1.3$) systems represent slow, marginal and fast cases, respectively. Figure 2 shows a schematic light curve by mutual transits.

Fig. 3 shows a slow case in circular motion, where we assume $R_s : R_p : R_m = 20 : 2 : 1$. We assume also the same mass density for the two transiting objects and hence obtain $a_p : a_m = 1 : 8$.

Eccentric orbit cases ($W = 6$ and $e_m = 0.3$) are shown by Figs. 4, 5 and 6 ($\omega_m = \pi/2$, 0 and $\pi/4$, respectively). Some parameters are chosen so that effects in the figures can be distinguished by eye, though such an event is unlikely to be detected by current observations as discussed later. For generating the ingress and egress of the various parts of the lightcurve, we do not use a linear interpolation but compute numerically the apparent overlap area between the objects. Here we assume the same configuration except for the observer’s line of sight. For simplicity, we take $t_0 = t_{CM} = 0$ in these figures.

These figures show also the transverse positions of transiting objects with time, which

would help us to understand the chronological changes in the light curves. In particular, it can be understood that such characteristic patterns appear only when two objects are in front of the star and one of them transits (or occults) the other.

3. Formulation for Parameter Determinations by Transit Method

3.1. Parameter determinations from transit observations alone

In all the above cases, the amount of decrease in light curves or the magnitude of fluctuations gives the ratios among the radii of the star and two faint objects (R_s, R_p, R_m). The decrease ratios in the apparent brightness due to transits by the planet and moon are written as

$$\Delta_p = \left(\frac{R_p}{R_s}\right)^2, \quad (12)$$

$$\Delta_m = \left(\frac{R_m}{R_s}\right)^2. \quad (13)$$

The stellar radius R_s (and mass M_S) are known for instance by its spectral type. Hence, the radii are expressed in terms of observables R_s, Δ_p and Δ_m as

$$R_p = R_s \sqrt{\Delta_p}, \quad (14)$$

$$R_m = R_s \sqrt{\Delta_m}. \quad (15)$$

We define the ratio between the brightness changes by the two objects as

$$\Delta \equiv \frac{\Delta_m}{\Delta_p}. \quad (16)$$

Circular Orbit and Orbital Inclination:

First, we discuss a circular orbit in order to simply explain our idea. For more rigorous treatment of eccentric orbits, please see below, where we will finally give expressions for determining the separation a_{pm} .

Behaviors of apparent light curves depend on W . Therefore, $a_{pm}n_m$ (as its ratio to v_{CM}) can be obtained (Sato and Asada 2009). Seager and Mallén-Ornelas (2003) presents an analytic solution of parameter determinations for a single transit in the circular orbit case. Their solution can be used for our case of mutual transits by a planet and moon in front of a host star. In our case, their equations are rewritten as follows. The duration of the ‘flat part’ of the transit (t_{Fm}) is described by

$$\sin\left(\frac{t_{Fm}\pi}{T_m}\right) = \frac{1}{a_{pm}\sin I_m} \sqrt{(R_p - R_m)^2 - (a_{pm}\cos I_m)^2}, \quad (17)$$

whereas the total transit duration (t_{Tm}) is done by

$$\sin\left(\frac{t_{Tm}\pi}{T_m}\right) = \frac{1}{a_{pm}\sin I_m} \sqrt{(R_p + R_m)^2 - (a_{pm}\cos I_m)^2}, \quad (18)$$

where I_m denotes the orbital inclination angle of the moon. By combining these equations, the impact parameter (b_{pm}) can be derived as

$$\begin{aligned} b_{pm} &\equiv \frac{a_{pm}}{R_p} \cos I_m \\ &= \sqrt{\frac{(1 - \sqrt{\Delta})^2 - [\sin^2(t_{Fm}\pi/T_m)/\sin^2(t_{Tm}\pi/T_m)](1 + \sqrt{\Delta})^2}{1 - [\sin^2(t_{Fm}\pi/T_m)/\sin^2(t_{Tm}\pi/T_m)]}}. \end{aligned} \quad (19)$$

The ratio a_{pm}/R_p can be derived directly from Eq. (18) as

$$\frac{a_{pm}}{R_p} = \sqrt{\frac{(1 + \sqrt{\Delta})^2 - b_{pm}^2[1 - \sin^2(t_{Tm}\pi/T_m)]}{\sin^2(t_{Tm}\pi/T_m)}}. \quad (20)$$

Therefore, one can obtain a_{pm} as $R_s \times (R_p/R_s) \times (a_{pm}/R_p)$.

With a_{pm} and n_m in hand, one can thus estimate the total mass of the binary by $GM_{tot} = n_m^2 a_{pm}^3$ from Kepler's third law, where G denotes the gravitational constant. The orbital velocity $a_{pm}n_m$ gives the mutual force between the binary.

If we assume also that the mass density is common for two objects constituting the binary (this may be reasonable especially for similar size objects as $R_p \sim R_m$), each mass is determined as $M_p = R_p^3(R_p^3 + R_m^3)^{-1}M_{tot}$ and $M_m = R_m^3(R_p^3 + R_m^3)^{-1}M_{tot}$, respectively. Therefore, the orbital radius of each body around the COM is obtained as $a_p = R_m^3(R_p^3 + R_m^3)^{-1}a_{pm}$ and $a_m = R_p^3(R_p^3 + R_m^3)^{-1}a_{pm}$, respectively. At this point, importantly, the two objects can be identified as a true binary ($a_p > R_p$) or planet-satellite system ($a_p < R_p$). However, a gaseous giant planet with a rocky satellite would exhibit largely different densities and this may be one of the most likely scenarios.

In a slow spin case, on the other hand, the apparent separation a_{\perp} (normal to our line of sight) is determined as $a_{\perp} = T_{12}v_{CM}$ from measuring the time lag T_{12} between the first and second transits because v_{CM} is known above (Sato and Asada 2009).

Eccentric Orbit and Edge-on Case:

Henceforth, we take account of the orbital eccentricity of a moon for an edge-on case. In this case, intervals between neighboring ‘‘hills’’ are not constant because of the eccentricity. However, a time duration between three successive ‘‘hills’’ is nothing but the orbital period of the moon. Therefore, one can measure the period T_m . We obtain n_m as

$$n_m = \frac{2\pi}{T_m}. \quad (21)$$

A key idea for determining the eccentricity is as follows. As for timescales, we have two observable ratios as T_2/T_1 and T_{12}/T_{21} . The former is the ratio between the widths of neighboring hills, whereas the latter is that between the transit intervals. On the other hand, we have two additional parameters e_m and ω_m to be determined. Importantly, the number of measurable ratios is the same as that of the parameters that we wish to determine. In principle, therefore, the above two ratios may allow us to determine the two parameters e_m and

ω_m , separately. This will be discussed in detail below.

To be more precise, the full width of a “hill” at top and bottom are expressed as (See also Figure 2)

$$T_{top} = \frac{2(R_p - R_m)}{V_f}, \quad (22)$$

$$T_{bottom} = \frac{2(R_p + R_m)}{V_f}. \quad (23)$$

Only for symmetric binaries ($R_p = R_m$), we have $T_{top} = 0$ and thus true spikes. Otherwise, truncated spikes (or “hills”) appear.

For the primary transit, where the moon moves in front of the planet, we have $f = \pi/2 - \omega_m$. From Eqs. (9), (22) and (23), therefore, we obtain

$$T_{1top} = \frac{2(R_p - R_m)}{a_{pm}n_m} \frac{\sqrt{1 - e_m^2}}{1 + e_m \sin \omega_m}, \quad (24)$$

$$T_{1bottom} = \frac{2(R_p + R_m)}{a_{pm}n_m} \frac{\sqrt{1 - e_m^2}}{1 + e_m \sin \omega_m}. \quad (25)$$

For the circular orbit $e_m = 0$, the second factors in the R.H.S. of these expressions become the unity and the first factors recover the case for $e_m = 0$ (See Sato and Asada 2009).

For the secondary transit, where the moon moves behind the planet, we have $f = 3\pi/2 - \omega_m$. From Eqs. (9), (22) and (23), therefore, we obtain

$$T_{2top} = \frac{2(R_p - R_m)}{a_{pm}n_m} \frac{\sqrt{1 - e_m^2}}{1 - e_m \sin \omega_m}, \quad (26)$$

$$T_{2bottom} = \frac{2(R_p + R_m)}{a_{pm}n_m} \frac{\sqrt{1 - e_m^2}}{1 - e_m \sin \omega_m}. \quad (27)$$

We immediately obtain from Eqs. (24), (25), (26) and (27),

$$\begin{aligned} T_r &\equiv \frac{T_{2top}}{T_{1top}} \\ &= \frac{T_{2bottom}}{T_{1bottom}} \\ &= \frac{1 + e_m \sin \omega_m}{1 - e_m \sin \omega_m}. \end{aligned} \quad (28)$$

Equation (28) is rewritten as

$$\begin{aligned} e_m \sin \omega_m &= \frac{T_r - 1}{T_r + 1} \\ &\equiv T_R, \end{aligned} \quad (29)$$

where the R.H.S. can be determined by observations alone. Once either e_m or ω_m is known, Eq. (29) determines the other.

Next, we consider the time interval between the primary and secondary transits. In

order to compute such an interval, one can use the Kepler's second law (the constant areal velocity). After lengthy but straightforward calculations, the area swept from the primary transit ($f = \pi/2 - \omega_m$) till the secondary ($f = 3\pi/2 - \omega_m$) becomes

$$S_{12} = a_m b_m \times \left[\frac{\pi}{2} + \arcsin H + \frac{1}{2} \sin(2 \arcsin H) \right], \quad (30)$$

where b_m denotes the semiminor axis of the moon's elliptic orbit and H is defined as

$$H = e_m \sqrt{\frac{\cot^2 \omega_m}{1 - e_m^2 + \cot^2 \omega_m}}. \quad (31)$$

By using Eq. (29) in Eq. (31) for eliminating $\cot \omega_m$, we obtain

$$H = \sqrt{\frac{e_m^2 - T_R^2}{1 - T_R^2}}. \quad (32)$$

It is convenient to use T_{12}/T instead of T_{12}/T_{21} , because T_{12}/T gives a simpler expression than T_{12}/T_{21} , which is used in the above explanation of the key idea. The total area is $S = \pi a_m b_m$. Therefore, we find

$$\begin{aligned} \frac{T_{12}}{T} &= \frac{S_{12}}{S} \\ &= \frac{1}{2} + \frac{1}{\pi} \arcsin H + \frac{1}{\pi} H \sqrt{\frac{1 - e_m^2}{1 - T_R^2}}. \end{aligned} \quad (33)$$

This includes e_m without ω_m . Hence by using this relation, one can determine separately the eccentricity by measuring the time intervals. We should note that Eq. (33) is valid even for a general case with a certain inclination angle.

Here, we consider a small eccentricity approximation, which may be useful for a quicker estimation of the parameters. For small e_m , Eq. (31) is expanded as

$$H = e_m \cos \omega_m + O(e_m^3). \quad (34)$$

Substitution of this into Eq. (33) gives us

$$\frac{T_{12}}{T_m} = \frac{1}{2} + \frac{2e_m}{\pi} \cos \omega_m + O(e_m^3). \quad (35)$$

The correction to the circular case ($T_{12}/T_m = 1/2$) is $2e_m \cos \omega_m / \pi \sim 0.7e_m \cos \omega_m$. Even for $\omega_m \sim 0$ for instance, it leads to seven percents for $e_m = 0.1$.

We define the difference between T_{12} and T_{21} as

$$\delta T \equiv T_{12} - T_{21}. \quad (36)$$

Replacement ω_m by $\omega_m + \pi$ changes Eq. (35) into

$$\frac{T_{21}}{T_m} = \frac{1}{2} - \frac{2e_m}{\pi} \cos \omega_m + O(e_m^3). \quad (37)$$

By using Eqs. (35) and (37), we obtain

$$e_m \cos \omega_m = \frac{\pi \delta T}{4T_m} + O(e^3). \quad (38)$$

Let us consider every cases separately.

(I) If and only if the L.H.S. of Eqs. (29) and (38) vanish, e_m does. This means a circular motion and thus the observer's direction ω_m becomes meaningless.

(II) For a case when the L.H.S. of Eq. (29) vanishes but that of Eq. (38) does not, we find $e_m \neq 0$ and $\sin \omega_m = 0$, namely

$$\omega_m = 0 \pmod{\pi}. \quad (39)$$

Eq. (38) immediately gives

$$e_m = \frac{\pi \delta T}{4T_m}. \quad (40)$$

Hence, the orbital eccentricity is determined.

(III) If the L.H.S. in Eq. (38) vanishes but that in (29) does not, we find $e_m \neq 0$ and $\cos \omega_m = 0$, namely

$$\omega_m = \frac{\pi}{2} \pmod{\pi}. \quad (41)$$

Eq. (29) immediately gives

$$e_m = T_R. \quad (42)$$

Hence, the orbital eccentricity is measured.

(VI) A general case in which the L.H.S. of neither Eqs. (29) nor (38) vanish: By dividing Eq. (38) by Eq. (29), we obtain

$$\cot \omega_m = \frac{\pi \delta T}{4 T_m T_R}, \quad (43)$$

where the R.H.S. can be determined by observations alone and hence this equation gives us the observer's direction ω_m . By substituting the determined ω_m into Eq. (29), one can find the value of the eccentricity.

Up to this point, e_m and ω_m both are determined. Eqs. (24) and (25) are rewritten as

$$\begin{aligned} a_{pm} &= \frac{T_m(R_p - R_m)}{\pi T_{1top}} \frac{\sqrt{1 - e_m^2}}{1 + e_m \sin \omega_m} \\ &= \frac{T_m(R_p - R_m)(T_{1top} + T_{2top})\sqrt{1 - e_m^2}}{2\pi T_{1top}T_{2top}} \\ &= \frac{(R_p - R_m)}{2\pi} \left(\frac{T_m}{T_{1top}} + \frac{T_m}{T_{2top}} \right) \sqrt{1 - e_m^2}, \\ a_{pm} &= \frac{T_m(R_p + R_m)}{\pi T_{1bottom}} \frac{\sqrt{1 - e_m^2}}{1 + e_m \sin \omega_m} \\ &= \frac{T_m(R_p + R_m)(T_{1bottom} + T_{2bottom})\sqrt{1 - e_m^2}}{2\pi T_{1bottom}T_{2bottom}} \end{aligned} \quad (44)$$

$$= \frac{(R_p + R_m)}{2\pi} \left(\frac{T_m}{T_{1bottom}} + \frac{T_m}{T_{2bottom}} \right) \sqrt{1 - e_m^2}, \quad (45)$$

respectively, where we used Eq. (29) If and only if $R_p = R_m$, we obtain $T_{1top} = T_{2top} = 0$ and Eq. (44) thus becomes undetermined, whereas Eq. (45) is still well-defined.

When one wishes to consider the secondary transit instead of the first, one can use

$$a_{pm} = \frac{T_m(R_p - R_m)}{\pi T_{2top}} \frac{\sqrt{1 - e_m^2}}{1 - e_m \sin \omega_m}, \quad (46)$$

$$a_{pm} = \frac{T_m(R_p + R_m)}{\pi T_{2bottom}} \frac{\sqrt{1 - e_m^2}}{1 - e_m \sin \omega_m}. \quad (47)$$

They are obtained by replacing ω_m with $\omega_m + \pi$ in Eqs. (44) and (45). By noting $T_{1top}(1 + T_R) = T_{2bottom}(1 - T_R)$ and $T_{2top}(1 + T_R) = T_{2bottom}(1 - T_R)$, one can show that Eqs. (46) and (47) agree with Eqs. (44) and (45), respectively. By using one of these expressions, we can thus measure the semimajor axis of the eccentric orbit. In terms of the decrease in apparent brightness, Eqs. (44) and (45) are written as

$$\frac{a_{pm}}{R_s} = \frac{(\sqrt{\Delta_p} - \sqrt{\Delta_m})}{2\pi} \left(\frac{T_m}{T_{1top}} + \frac{T_m}{T_{2top}} \right) \sqrt{1 - e_m^2}, \quad (48)$$

$$\frac{a_{pm}}{R_s} = \frac{(\sqrt{\Delta_p} + \sqrt{\Delta_m})}{2\pi} \left(\frac{T_m}{T_{1bottom}} + \frac{T_m}{T_{2bottom}} \right) \sqrt{1 - e_m^2}, \quad (49)$$

where we used Eqs. (14) and (15).

Determination of the semimajor axis is sensitive to measurement errors in the widths of the hills. This statement can be proven by using Eq. (49). For simplicity, we assume $\Delta_p \sim \Delta_m \sim \Delta$ and $T_{1bottom} \sim T_{2bottom} \sim T_{bottom}$, so that Eq. (49) can be reduced to

$$a_{pm} \sim \frac{2}{\pi} R_s \sqrt{\Delta} \frac{T_m}{T_{bottom}} \sqrt{1 - e_m^2}. \quad (50)$$

The logarithmic derivative of this becomes

$$\frac{da_{pm}}{a_{pm}} \sim \frac{dR_s}{R_s} + \frac{d\Delta}{2\Delta} + \frac{dT_m}{T_m} - \frac{dT_{bottom}}{T_{bottom}} - \frac{e_m de_m}{(1 - e_m^2)}. \quad (51)$$

We focus on dT_m/T_m and dT_{bottom}/T_{bottom} , because we can expect much more accurate measurements for R_s and Δ , and the last term involving e_m may be relatively small ($e_m < 1$ and $de_m < 1$). Time resolution in observations seems $dT_m \sim dT_{bottom}$, while $T_m \gg T_{bottom}$. Therefore, $dT_m/T_m \ll dT_{bottom}/T_{bottom}$, which means that accurate measurements of T_{bottom} are crucial for the determination of a_{pm} .

Figure 7 shows a flow chart of the parameter determinations that are discussed above. The above formulation for parameter determinations actually recovers the correct values in Figs. 4-6. In the numerical examples, the original parameters are retrieved within twenty percents.

Eccentric Orbit and Orbital Inclination:

Figure 8 shows a difference between light curves for the edge-on ($I_m = 90$ deg.) and an inclination case ($I_m = 88$ deg.). Let z -axis denote the axis normal to the x -axis on the celestial sphere. We define the distance of a ‘moon’ from the z -axis at the initial time of the mutual transit as

$$s_b = \sqrt{(R_p + R_m)^2 - \left(\frac{a_{pm}(1 - e_m^2)}{1 + e_m \cos f}\right)^2} \cos^2 I_m, \quad (52)$$

where the subscript b means that the quantity is related with $T_{1bottom}$ and $T_{2bottom}$ as shown below (See also Fig. 9). Similarly, when the ‘flat part’ of the spike in light curves starts (or ends), we define the distance of a moon from the z -axis at this epoch as

$$s_t = \sqrt{(R_p - R_m)^2 - \left(\frac{a_{pm}(1 - e_m^2)}{1 + e_m \cos f}\right)^2} \cos^2 I_m, \quad (53)$$

where the subscript t means that the quantity is related with T_{1top} and T_{2top} as shown below.

Therefore, we obtain the duration T_{top} as

$$T_{top} = \frac{2s_t}{V_f}, \quad (54)$$

where V_f is given by Eq. (9). For the primary transit ($f = \pi/2 - \omega_m$), we thus obtain

$$T_{1top} = \frac{2s_{t1}\sqrt{1 - e_m^2}}{a_{pm}n_m(1 + e_m \sin \omega_m)}, \quad (55)$$

whereas for the secondary ($f = 3\pi/2 - \omega_m$), we have

$$T_{2top} = \frac{2s_{t2}\sqrt{1 - e_m^2}}{a_{pm}n_m(1 - e_m \sin \omega_m)}. \quad (56)$$

Here, we define s_{t1} and s_{t2} as

$$s_{t1} = \sqrt{(R_p - R_m)^2 - \left(\frac{a_{pm}(1 - e_m^2)}{1 + e_m \sin \omega_m}\right)^2} \cos^2 I_m, \quad (57)$$

$$s_{t2} = \sqrt{(R_p - R_m)^2 - \left(\frac{a_{pm}(1 - e_m^2)}{1 - e_m \sin \omega_m}\right)^2} \cos^2 I_m. \quad (58)$$

In the similar manner, we obtain the width of the spikes at the bottom as

$$T_{bottom} = \frac{2s_b}{V_f}. \quad (59)$$

For the primary transit ($f = \pi/2 - \omega_m$), we thus obtain

$$T_{1bottom} = \frac{2s_{b1}\sqrt{1 - e_m^2}}{a_{pm}n_m(1 + e_m \sin \omega_m)}, \quad (60)$$

whereas for the secondary ($f = 3\pi/2 - \omega_m$), we have

$$T_{2bottom} = \frac{2s_{b2}\sqrt{1 - e_m^2}}{a_{pm}n_m(1 - e_m \sin \omega_m)}, \quad (61)$$

where we define s_{b1} and s_{b2} as

$$s_{b1} = \sqrt{(R_p + R_m)^2 - \left(\frac{a_{pm}(1 - e_m^2)}{1 + e_m \sin \omega_m}\right)^2 \cos^2 I_m}, \quad (62)$$

$$s_{b2} = \sqrt{(R_p + R_m)^2 - \left(\frac{a_{pm}(1 - e_m^2)}{1 - e_m \sin \omega_m}\right)^2 \cos^2 I_m}. \quad (63)$$

Because of the orbital inclination, we have to consider T_{top} and T_{bottom} , separately. We define the ratios as

$$T_{rtop} \equiv \frac{T_{2top}}{T_{1top}}, \quad (64)$$

and

$$T_{rbottom} \equiv \frac{T_{2bottom}}{T_{1bottom}}. \quad (65)$$

Substitutions of Eqs. (55), (56), (60), (61) into these ratios lead to

$$T_{rtop} = \frac{s_{t2}}{s_{t1}} \frac{1 + e_m \sin \omega_m}{1 - e_m \sin \omega_m}, \quad (66)$$

$$T_{rbottom} = \frac{s_{b2}}{s_{b1}} \frac{1 + e_m \sin \omega_m}{1 - e_m \sin \omega_m}. \quad (67)$$

For the edge-on case ($I_m = 90$ deg.), we obtain $s_{t2}/s_{t1} = s_{b2}/s_{b1} = 1$. Then, we have $T_{rtop} = T_{rbottom}$. For a general case ($I_m \neq 90$ deg.), on the other hand, we find $T_{rtop} \neq T_{rbottom}$. We thus expect that a ratio between them will give us the information about the orbital inclination. The ratio is

$$\frac{T_{rtop}}{T_{rbottom}} = \frac{s_{t2} s_{b1}}{s_{t1} s_{b2}}. \quad (68)$$

The L.H.S. can be measured by observations.

There are four unknown quantities a_{pm} , e_m , I_m and ω_m . We have four equations of (66), (67), (68) and the last one that can be chosen out of (55), (56), (60) and (61). Therefore, one can determine the quantities a_{pm} , e_m , I_m and ω_m by using these equations for observations. For practical observations, data fittings at the slope of light curves are used, instead of transit durations, for determinations of the orbital inclination angle (Charbonneau et al. 2000). Nevertheless, an analytic solution is necessarily worthwhile to understand the properties of a given physical system, even when numerical fits are in practice the best way to determine the system parameters.

A partial transit occurs if the apparent impact parameter of the moon is in $(R_p - R_m, R_p + R_m)$. For the primary transit ($f = \pi/2 - \omega_m$), it occurs if the orbital inclination angle satisfies

$$\frac{R_p - R_m}{a_{pm}} \frac{1 + e_m \sin \omega_m}{1 - e_m^2} < \cos I_m < \frac{R_p + R_m}{a_{pm}} \frac{1 + e_m \sin \omega_m}{1 - e_m^2}. \quad (69)$$

For the secondary one ($f = 3\pi/2 - \omega_m$), the condition of a partial transit becomes

$$\frac{R_p - R_m}{a_{pm}} \frac{1 - e_m \sin \omega_m}{1 - e_m^2} < \cos I_m < \frac{R_p + R_m}{a_{pm}} \frac{1 - e_m \sin \omega_m}{1 - e_m^2}. \quad (70)$$

Such a partial transit by a moon orbiting a host planet produces a ‘U’-shaped spike in light curves (See Fig. 10).

3.2. Timescales and brightness changes

We have presented a formalism for parameter determinations. Before closing this section, let us make brief comments on typical timescales and amplitudes in the brightness changes.

The timescale of a brightness change due to a giant planet is about

$$\frac{R_p}{a_{pm}n_m} \sim 5 \times 10^3 \left(\frac{R_p}{5 \times 10^4 \text{km}} \frac{10 \text{km/s}}{a_{pm}n_m} \right) \text{sec.} \quad (71)$$

Therefore, *detections* of such fluctuations due to mutual transits of extrasolar planet-moon systems require frequent observations, say every hour. Furthermore, higher frequency (e.g., every ten minutes) is necessary for parameter *estimations* of the system.

Let us mention a connection of the present result with space telescopes in operation. Decrease in apparent luminosity due to the secondary planet is $O(R_m^2/R_s^2)$. Besides the time resolution (or observation frequency) and mission lifetimes, detection limits by *COROT* with the achieved accuracy of photometric measurements (700 ppm in one hour) could put $R_m/R_s \sim 2 \times 10^{-2}$. The nominal integration time is 32 sec. but co-added over 8.5 min. except for 1000 selected targets for which the nominal sampling is preserved. By the *Kepler* mission with expected 20 ppm differential sensitivity for solar-like stars with $m_V = 12$, the lower limit will be reduced to $R_m/R_s \sim 4 \times 10^{-3}$. An analogy of the Earth-Moon ($R_m/R_s \sim 2.5 \times 10^{-3}$, $W \sim 0.03$) and Jupiter-Ganymede ($R_m/R_s \sim 4 \times 10^{-3}$, $W \sim 0.8$) will be marginally detectable. Observations both with high frequency (at least during the time of transits) and with good photometric sensitivity are desired for future detections of mutual transits.

3.3. Dynamical limit and constraints on W

For Roche limit, we have

$$a_{pm} < \beta R_H, \quad (72)$$

where β denotes a numerical coefficient $0 < \beta < 1$ and R_H is Hill radius (See Domingos et al. 2006 for more detailed stability arguments by numerical computations). For simplicity, we assume $M_s \gg M_p \gg M_m$. Then, we have $a_{pm} \approx a_m$ and R_H is approximated as

$$R_H = \left(\frac{M_p}{3M_s} \right)^{1/3} d_p, \quad (73)$$

where M_s denotes a host star mass and d_p denotes the orbital radius of a planet orbiting the star. Kepler’s third law gives $a_{pm}n_m$ and v_{CM} as

$$a_{pm}n_m = \sqrt{\frac{GM_p}{a_m}}, \quad (74)$$

$$v_{CM} = \sqrt{\frac{GM_s}{d_p}}. \quad (75)$$

Combining these relations, therefore, we find

$$W > 3^{1/6} \beta^{-1/2} \left(\frac{M_p}{M_s} \right)^{1/3}. \quad (76)$$

If one assumes $M_p \sim M_J$ (Jupiter mass), we obtain $W > 10^{-1}$. This lower bound is less severe. On the other hand, there is a stringent constraint that the moon's closest approach r_{min} cannot be within the planetary radius. We thus have

$$a_m > \frac{r_{min}}{1 - e_m}. \quad (77)$$

This leads to

$$W < \sqrt{\frac{M_p}{M_s} \frac{d_p}{r_{min}}} (1 - e_m). \quad (78)$$

If one assumes the jovian mass and radius (R_J), this is rewritten as

$$W < 1.4 \left(\frac{d_p}{1\text{AU}} \right)^{1/2} \left(\frac{M_\odot}{M_s} \right)^{1/2} \left(\frac{M_J}{M_p} \right)^{1/2} \left(\frac{R_J}{r_{min}} \right)^{1/2} (1 - e_m)^{1/2}. \quad (79)$$

For $W = 6$ and $e_m = 0.3$, we obtain $d_p > 25$ AU. Namely, a planet with a long orbital period $T_p > 125$ years is required. Kepler mission for several years is unlikely to see a transit by such a long period planet.

Next, we consider a constraint that a mutual transit can occur. The transit duration for a planet in circular orbit is

$$D \sim \frac{T_p R_s}{\pi d_p}, \quad (80)$$

where we assume the maximum duration by taking the vanishing impact parameter (See Seager and Mallén-Ornelas for a more accurate form). As this limiting case for the Roche limit, we obtain the fastest case of a 'moon' as

$$a_m \sim \beta \left(\frac{M_p}{3M_s} \right)^{1/3} d_p. \quad (81)$$

Using the Kepler's third law, this leads to

$$T_m \sim \left(\frac{\beta^3}{3} \right)^{1/2} T_p. \quad (82)$$

For our fast case, we require $T_m < D$, which gives a bound on β as

$$\beta < 3^{1/3} \left(\frac{R_s}{\pi d_p} \right)^{2/3}. \quad (83)$$

We substitute this into β of Eq. (76) so that we can obtain

$$\begin{aligned} W &> \left(\frac{\pi d_p}{R_s} \right)^{1/3} \left(\frac{M_p}{M_s} \right)^{1/3} \\ &\sim 1.5 \left(\frac{d_p}{d_J} \right)^{1/3} \left(\frac{R_\odot}{R_s} \right)^{1/3} \left(\frac{M_p}{M_J} \right)^{1/3} \left(\frac{M_\odot}{M_s} \right)^{1/3} \end{aligned}$$

$$\sim 0.9 \left(\frac{T_p}{1\text{year}} \right)^{2/9} \left(\frac{R_\odot}{R_s} \right)^{1/3} \left(\frac{M_p}{M_J} \right)^{1/3} \left(\frac{M_\odot}{M_s} \right)^{1/3}, \quad (84)$$

where d_J denotes the mean orbital radius of the Jupiter.

On the other hand, the dynamical arguments put an upper bound by Eq. (79). This is rewritten as

$$W < 1.4 \left(\frac{T_p}{1\text{year}} \right)^{1/3} \left(\frac{M_\odot}{M_s} \right)^{1/2} \left(\frac{M_J}{M_p} \right)^{1/2} \left(\frac{R_J}{r_{min}} \right)^{1/2} (1 - e_m)^{1/2}. \quad (85)$$

Therefore, there exists a narrow band as shown by Fig. 11. Outside this range, the proposed method cannot work.

4. Conclusion

We have shown that light curves by mutual transits of an extrasolar planet with a ‘moon’ depend on the moon’s orbital eccentricity, especially for small separation (fast) cases, in which occultation of one faint object by the other transiting a parent star causes an apparent increase in light curves and such characteristic fluctuations with the same height repeatedly appear. We have also presented a formulation for determining the parameters such as the orbital eccentricity, inclination, semimajor axis and the direction of the observer’s line of sight. This will be useful for probing the nature of the transiting planet-moon system.

When actual light curves are analyzed, we should incorporate (1) photometric corrections such as limb darkenings, and (2) perturbations as three (or more)-body gravitating interactions (e.g., Danby 1988, Murray and Dermott 2000).

We would like to thank the referee for invaluable comments on the manuscript. We would like to thank S. Ida, S. Inutsuka, E. Kokubo and Y. Suto for stimulating conversations and encouragements. This work was supported in part (H.A) by a Japanese Grant-in-Aid for Scientific Research from the Ministry of Education, No. 21540252.

References

- Aitken, R. G. 1964 *The Binary Stars* (NY: Dover)
- Binnendijk, L. 1960 *Properties of Double Stars* (Philadelphia: University of Pennsylvania Press)
- Cabrera, J., & Schneider, J. 2007, *A&A*, 464, 1133
- Canup, R. M., & Ward, W. R. 2006, *Nature*, 441, 834
- Charbonneau, D., Brown, T. M., Latham, D. W., & Mayor, M., 2000, *ApJ*, 529, L45
- Danby, J. M. A., 1988, *Fundamentals of Celestial Mechanics* (VA, William-Bell)
- Deeg, H. J., et al., 1998, *A&A*, 338, 479
- Deeg, H. J., Doyle, L. R., Kozhevnikov, V. P., Blue, J. E., Martin, E. L., Schneider, J., 2000, *A&A*, 358, L5
- Deming, D., Seager, S., Richardson, L. J., & Harrington, J., 2005, *Nature*, 434, 740

Domingos, R. C., Winter, O. C., & Yokoyama, T. 2006, MNRAS, 373, 1227
Doyle, L. R., et al., 2000, ApJ, 535, 338
Gaudi, B. S., & Winn, J. N., 2007, ApJ, 655, 550
Jewitt, D., & Haghighipour, N. 2007, ARAA, 45, 261
Jewitt, D., & Sheppard, S. 2005, Space. Sci. Rev., 116, 441
Kipping, D. M. 2009a, MNRAS, 392, 181
Kipping, D. M. 2009b, arXiv:0904.2565
Léger, A., et al. 2009, A&A, 506, 287L
Murray, C. D., Dermott, S. F., 2000, *Solar system dynamics* (Cambridge, Cambridge U. Press)
Narita, N., et al. 2007, PASJ, 59, 763
Narita, N., Sato, B., Ohshima, O., & Winn, J. N. 2008, PASJ, 60, L1
Ohta, Y., Taruya, A., & Suto, Y. 2005, ApJ, 622, 1118
Queloz, D., et al. 2009, A&A, 506, 303
Sartoretti, P., & Schneider, J. 1999, A&AS, 134, 553
Sato, M., & Asada, H. 2009, PASJ, 61, L29
Seager, S., & Mallén-Ornelas, G. 2003, ApJ, 585, 1038
Simon, A., Szatmáry, K., & Szabó, G. M. 2007, A&A, 470, 727
Szabó, G. M., Szatmáry, K., Divéki, Z., & Simon, A. 2006, A&A, 450, 395
Williams, D. M., Kasting, J. F., & Wade, R. A. 1997, Nature, 385, 234
Winn, J. N., et al. 2005, ApJ, 631, 1215

Table 1. List of quantities characterizing a system in this paper.

Symbol	Definition
T_m	Orbital period of an extrasolar ‘moon’ around a planet
n_m	Mean motion of a moon ($= 2\pi/T_m$)
a_m	Semimajor axis of a moon’s orbit w.r.t. a planet-moon’s center of mass
a_p	Semimajor axis of a planet’s orbit w.r.t. a planet-moon’s center of mass
a_{pm}	Semimajor axis of a moon’s orbit around a planet ($= a_p + a_m$)
a_{\perp}	Apparent separation of a planet-moon system
R_s	Radius of a host star
R_p	Radius of a planet
R_m	Radius of a moon
M_p	Mass of a planet
M_m	Mass of a moon
M_{tot}	$M_p + M_m$
x_{CM}	Transverse position of a planet-moon’s center of mass
v_{CM}	Transverse velocity of a planet-moon’s center of mass
x_p	Transverse position of a planet
x_m	Transverse position of a moon
e	Orbital eccentricity of the moon
t_0	Time of periastron passage of the moon
ω_m	Argument of pericenter of the moon
t_{CM}	Time when the planet-moon’s center of mass passes across the star’s center
Δ_p	Decrease rate in apparent brightness due to the planet transit
Δ_m	Decrease rate in apparent brightness due to the moon transit
T_{1top}	Time duration: width of a hill’s top at the primary transit in light curves
$T_{1bottom}$	Time duration: width of a hill’s bottom at the primary transit in light curves
T_{2top}	Time duration: width of a hill’s top at the secondary transit in light curves
$T_{2bottom}$	Time duration: width of a hill’s bottom at the secondary transit in light curves
T_{12}	Time lag from the first transit to the secondary
T_{21}	Time lag from the secondary transit to the first
δT	$T_{12} - T_{21}$

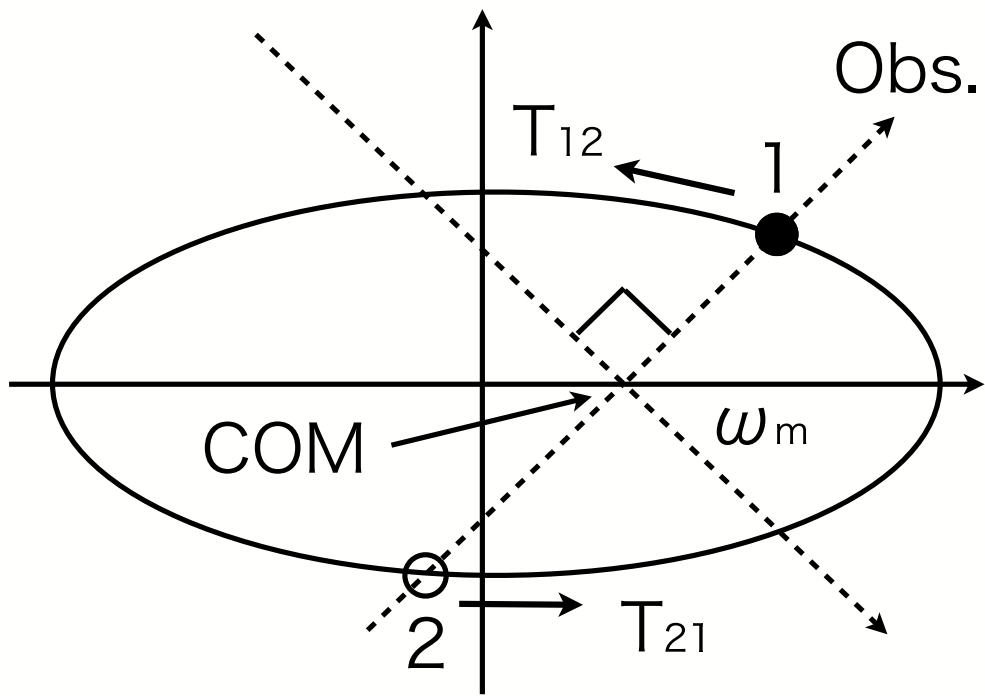


Fig. 1. Direction of the line of sight. It is denoted as ω_m , which is the argument of pericenter.

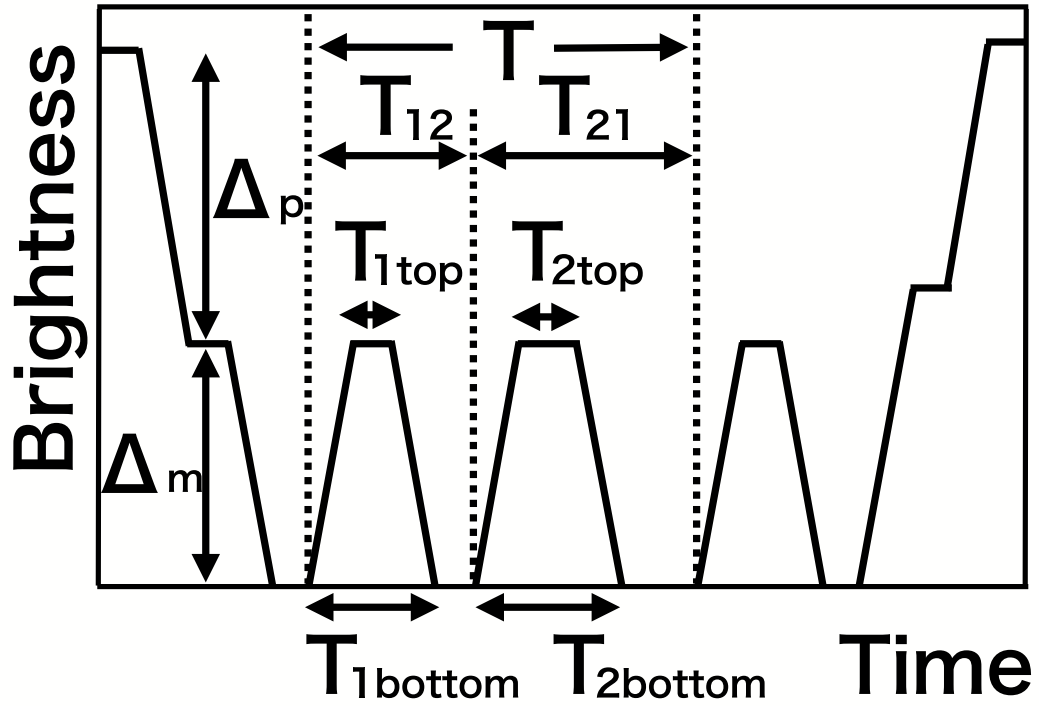


Fig. 2. Schematic figure of a light curve due to a mutually transiting planet and moon in front of their host star.

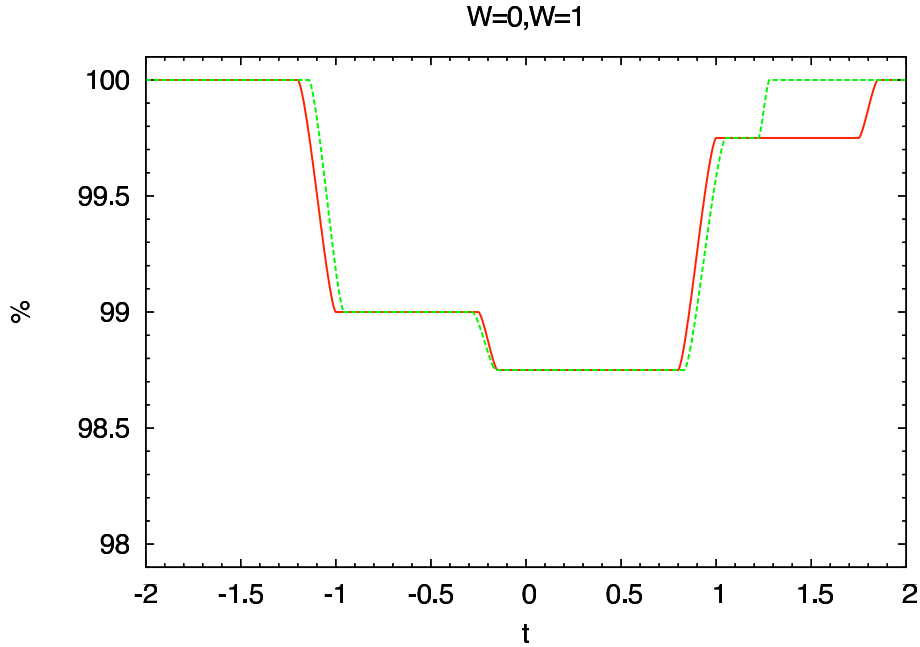


Fig. 3. Light curves: Solid red one denotes the zero limit of a ‘moon’ orbital motion as a reference ($W \equiv a_{pm}n_m/v_{CM} = 0$). Dashed green one is a marginal spin case (large separation) for $W = 1$ (Sato and Asada, 2009). The vertical axis denotes the apparent luminosity (in percents). The horizontal one is time in units of the half crossing time of the star by the COM of the binary, defined as R_s/v_{CM} . If one takes $M_s = M_\odot$, $R_s = R_\odot$ and $v_{CM} = 30$ km/s (namely, 1 AU distance from the host star), $t = 1$ corresponds to ≈ 6 hours. For simplicity, we assume the binary with a common mass density, a radius ratio as $R_s : R_p : R_m = 20 : 2 : 1$, and $a_{pm}/R_s = 0.9$.

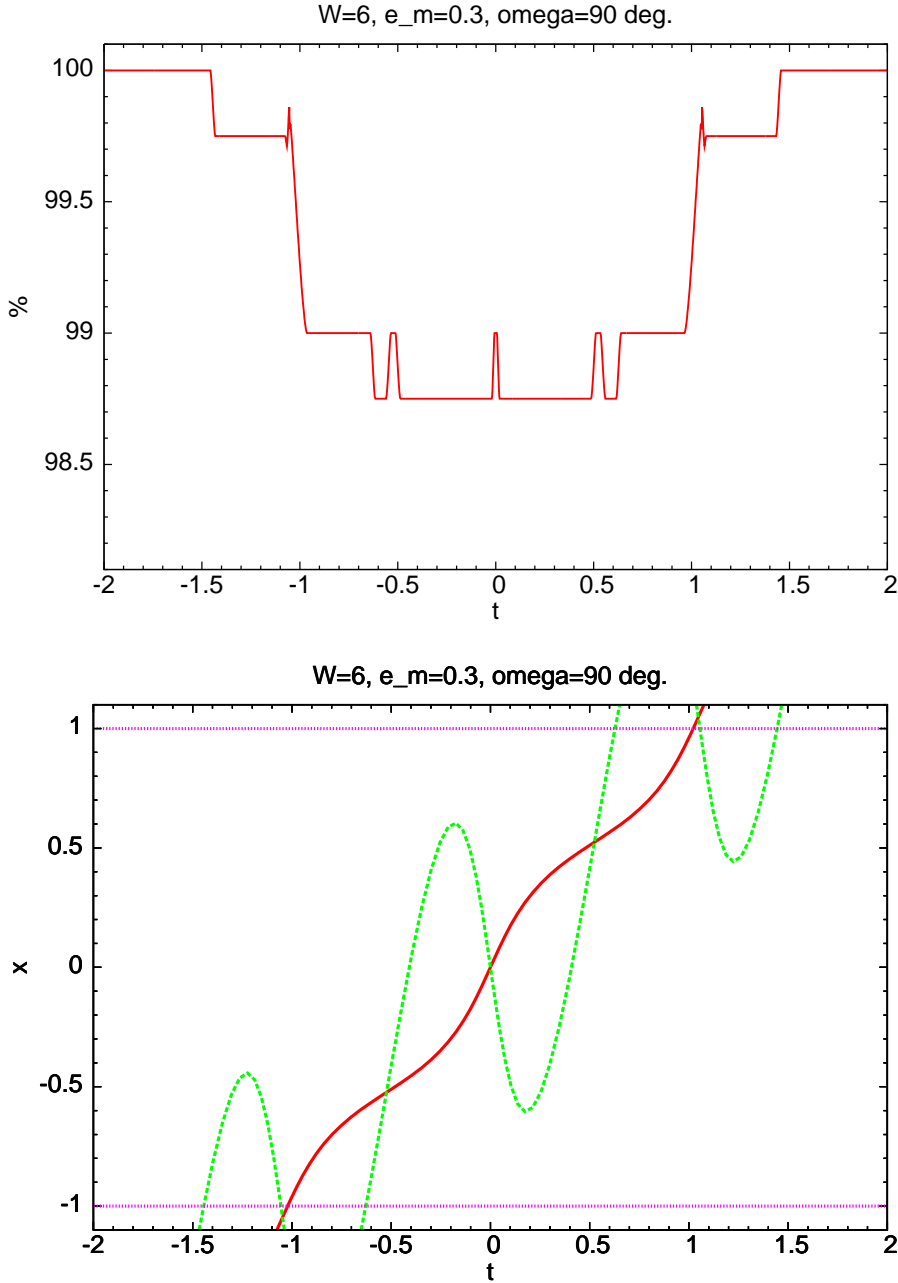


Fig. 4. Top panel: a light curve for a fast case (small separation) as $W = 6$ and $e_m = 0.3$. The radius and separation are the same as those in Fig. 3. The observer’s direction is $\omega_m = \pi/2$. Brightness fluctuations appear with $T_{1top}/T_m = 0.013$, $T_{1bottom}/T_m = 0.022$, $T_{2top}/T_m = 0.039$, $T_{2bottom}/T_m = 0.067$, $T_{12}/T_m = 0.51$ and $T_{21}/T_m = 0.49$ (normalized by T_m , the orbital period of the moon: $T_m = T_{12} + T_{21}$). We obtain $T_r \sim 1.7$ from Eq. (29) and thus $e_m \sin \omega_m \sim 0.3$, whereas Eq. (38) approximately gives us $e_m \cos \omega_m \sim 0$. Therefore, we recover well the parameters as $e_m \sim 0.3$ and $\omega_m \sim \pi/2$, even in the linear approximation in e_m . Finally, Eq. (49) tells $a_{pm}/R_s \sim 0.9$. Bottom panel: motion of each body in the direction of x normalized by R_s (solid red for the primary and dotted green for the secondary). When one faint object transits or occults the other in front of the host star, mutual transits occur and a ‘hill’ appears in the light curve.

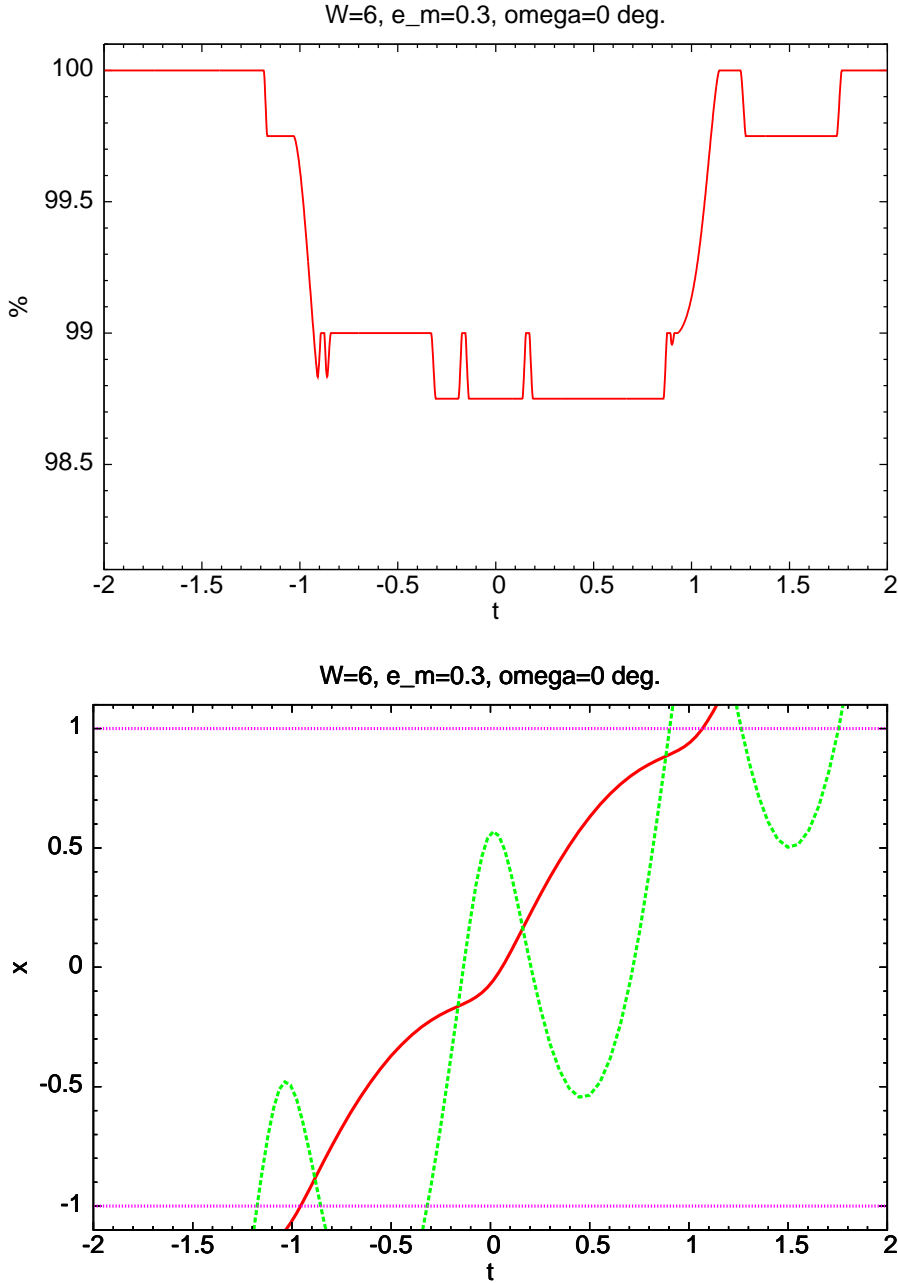


Fig. 5. Top panel: a light curve for all the parameters same as those in Fig. 4, except for the observer's direction as $\omega_m = 0$. Brightness fluctuations appear with $T_{1top}/T_m = 0.018$, $T_{1bottom}/T_m = 0.018$, $T_{2top}/T_m = 0.050$, $T_{2bottom}/T_m = 0.050$, $T_{12}/T_m = 0.69$ and $T_{21}/T_m = 0.31$. We obtain $T_r \sim 1.0$ from Eq. (29) and thus $e_m \sin \omega_m \sim 0$, whereas Eq. (38) approximately gives us $e_m \cos \omega_m \sim 0.3$. Therefore, we recover well the parameters as $e_m \sim 0.3$ and $\omega_m \sim 0$, even in the linear approximation in e_m . Finally, Eq. (49) tells $a_{pm}/R_s \sim 0.9$. Bottom panel: motion of each body (solid red for the primary and dotted green for the secondary).

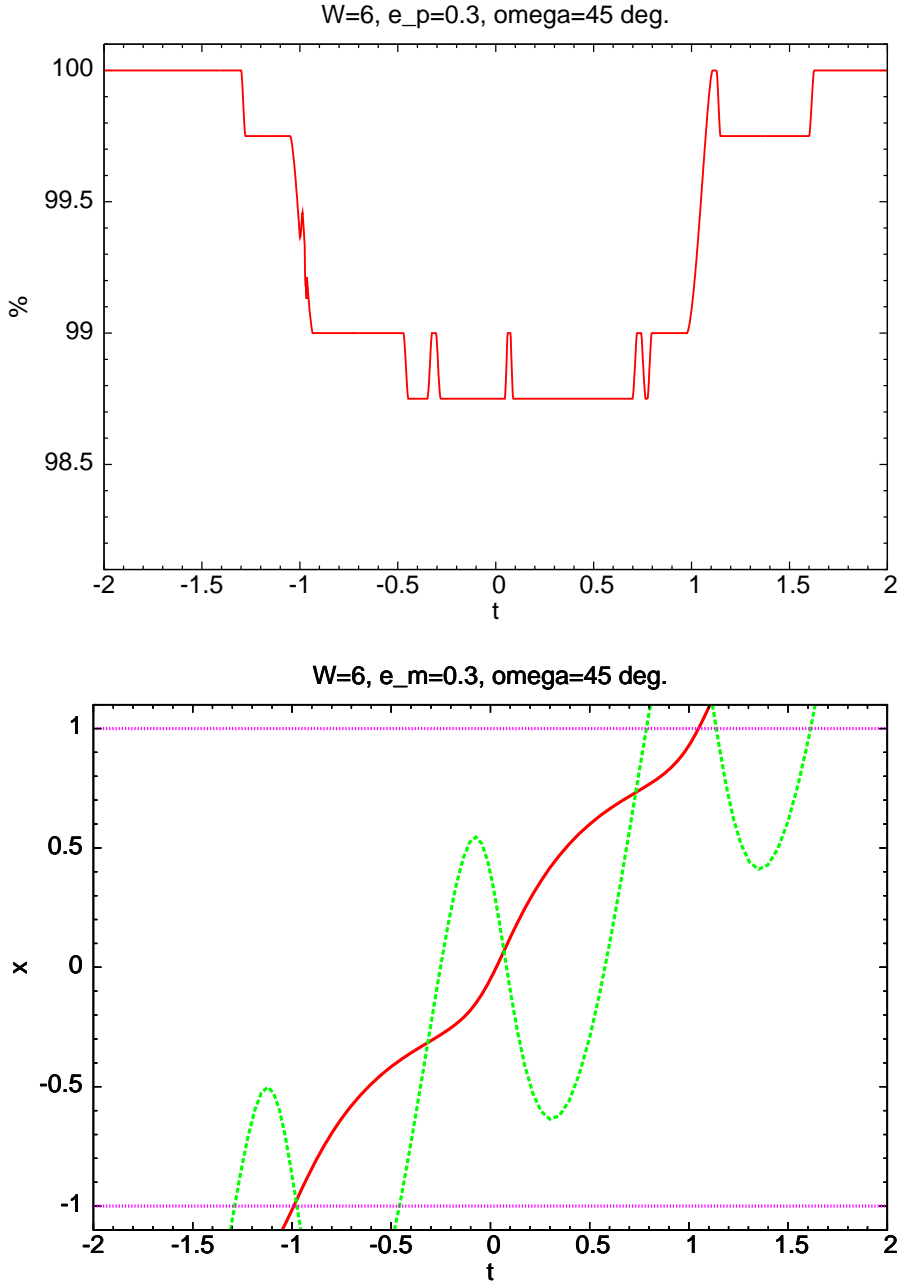


Fig. 6. Top panel: a light curve for all the parameters same as those in Fig. 4, except for the observer's direction as $\omega_m = \pi/4$. Brightness fluctuations appear with $T_{1top}/T_m = 0.015$, $T_{1bottom}/T_m = 0.022$, $T_{2top}/T_m = 0.041$, $T_{2bottom}/T_m = 0.062$, $T_{12}/T_m = 0.62$ and $T_{21}/T_m = 0.38$. We obtain $T_r \sim 1.5$ from Eq. (29) and thus $e_m \sin \omega_m \sim 0.2$, whereas Eq. (38) approximately gives us $e_m \cos \omega_m \sim 0.2$. Therefore, we recover well the parameters as $e_m \sim 0.3$ and $\omega_m \sim \pi/4$, even in the linear approximation in e_m . Finally, Eq. (49) tells $a_{pm}/R_s \sim 0.9$. Bottom panel: motion of each body (solid red for the primary and dotted green for the secondary).

Brightness changes

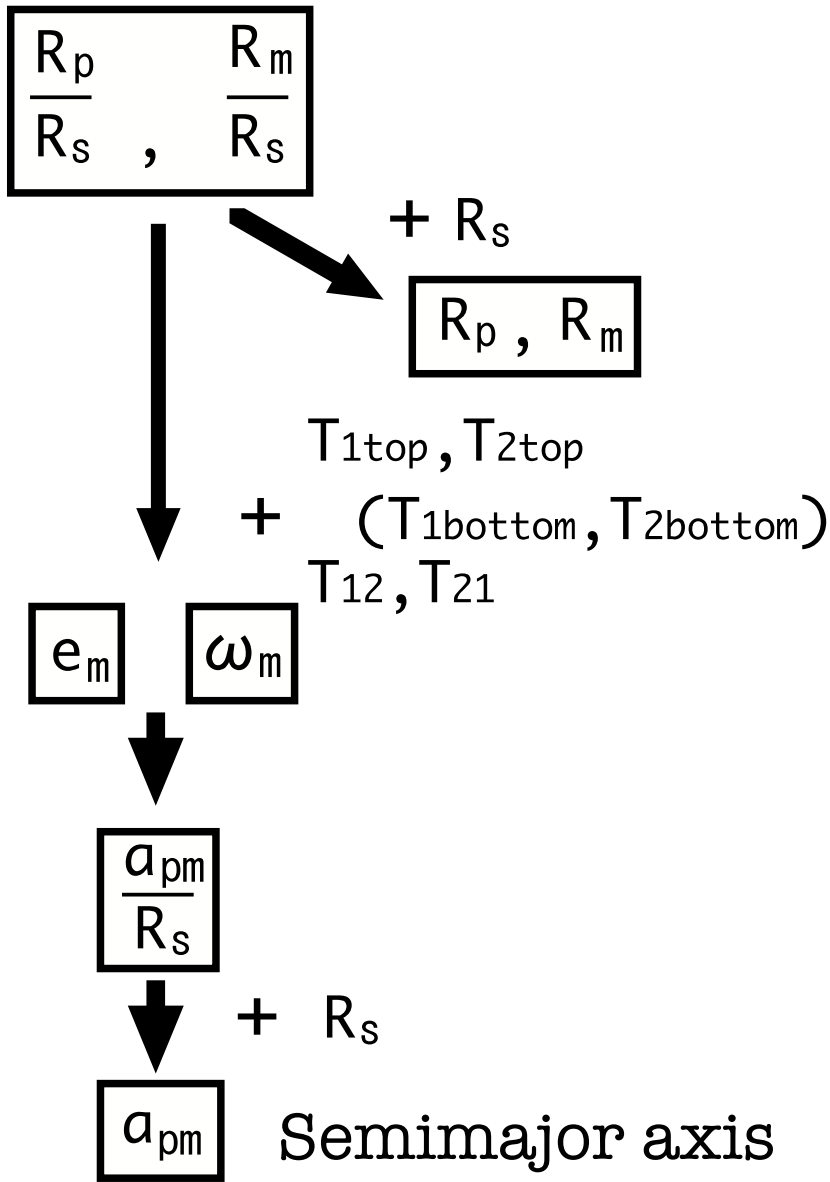


Fig. 7. Flow chart of parameter determinations. Starting from measurements of brightness changes, the semimajor axis a_{pm} can be finally determined for a fast case.

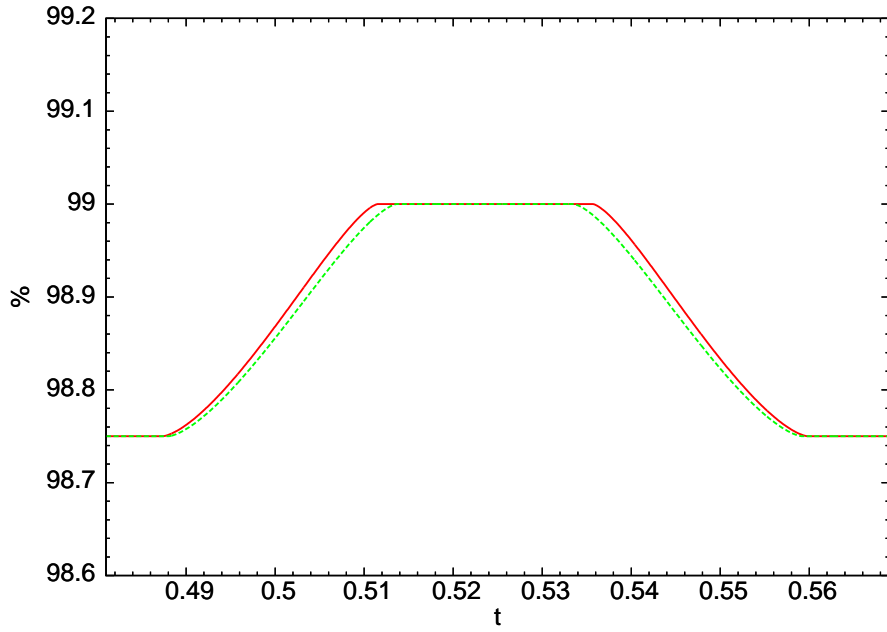


Fig. 8. Difference in light curves due to orbital inclinations of a ‘moon’. All parameters but for the inclination angle are the same as those in Fig. 4. The solid (red) curve denotes $I_m = 90$ degree case, while the dashed (green) one means a case of $I_m = 88$ deg. Because of the orbital inclination, the duration of a mutual transit by the satellite is shortened.

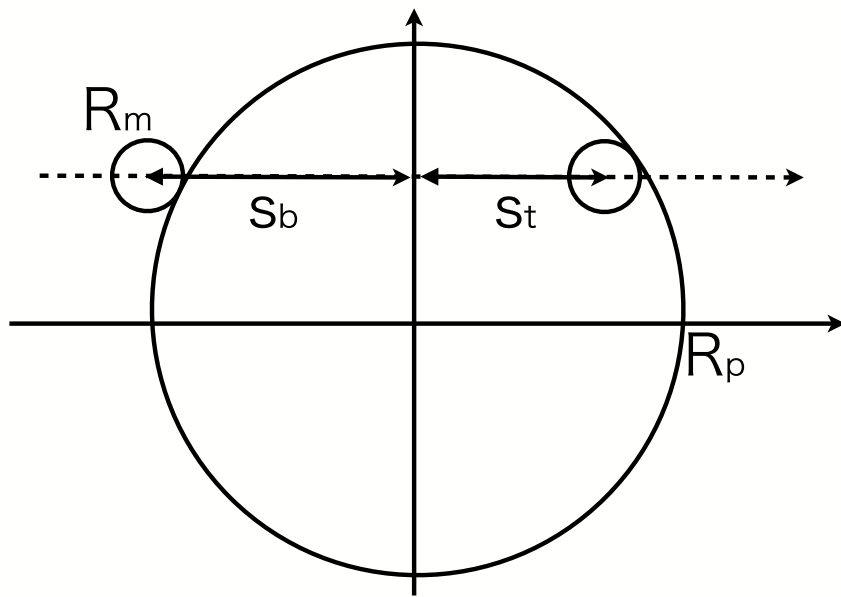


Fig. 9. Definition of s_b and s_t : The total transit duration T_{bottom} is given by s_b , whereas the ‘flat part’ of the hill T_{top} is done by s_t .

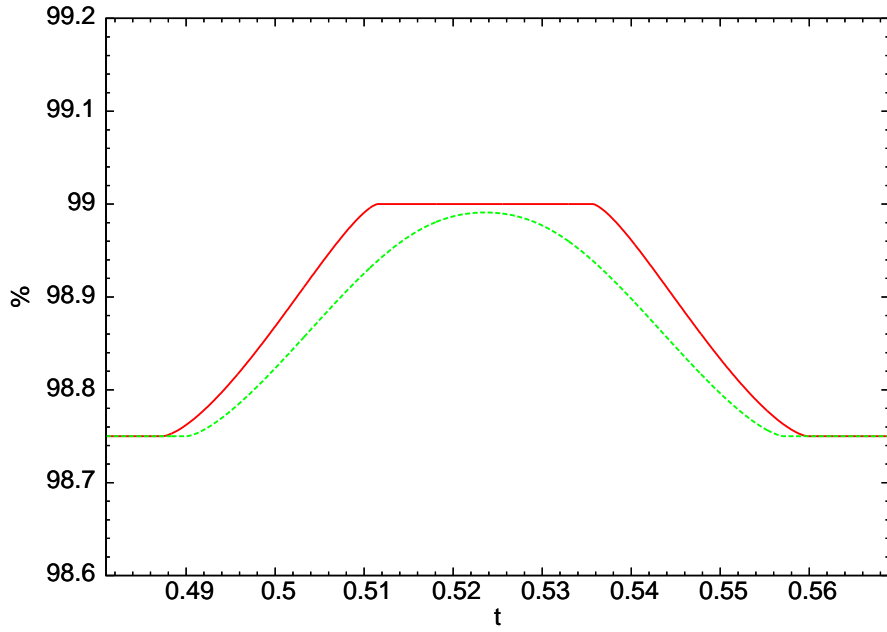


Fig. 10. Light curve by a partial mutual transit of a satellite. All parameters but for the inclination angle are the same as those in Fig. 4. The solid (red) curve denotes $I_m = 90$ degree case, while the dashed (green) one means a case of $I_m = 86$ degree for a partial transit. Such a partial transit case produces a ‘U’-shaped hill in light curves.

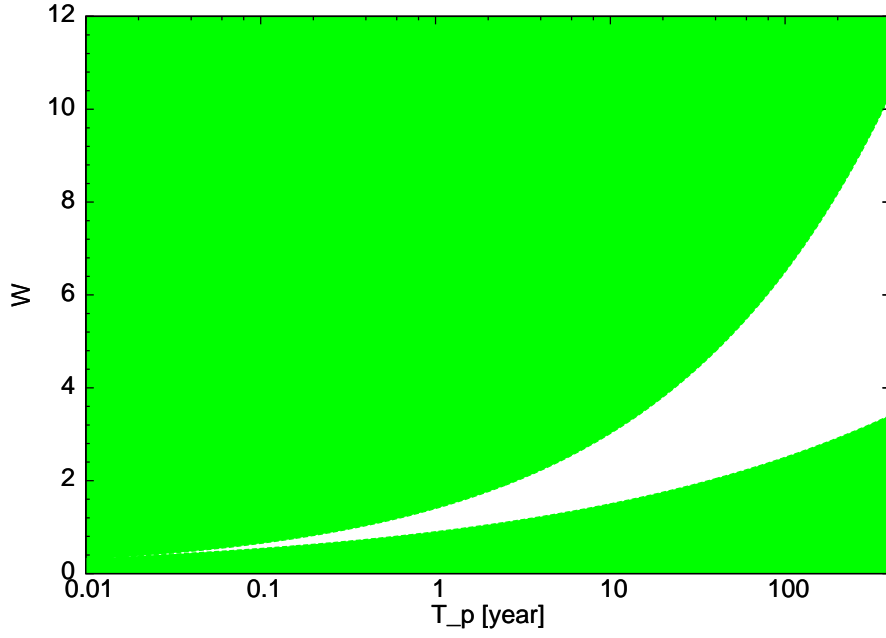


Fig. 11. Possible bound on W and T_p . Here, we assume $M_s = M_\odot$, $R_s = R_\odot$, $M_p = M_J$, $r_{min} = R_J$ and $e_m = 0$. The shaded (green) region denotes prohibited regions of the parameters that are constrained by Eqs. (84) and (85).